J Mater Sci (2007) 42:8986–8994
DOI 10.1007/s10853-007-1831-3

Time-dependant intercellular delamination of human stratum corneum

Kenneth S. Wu · James Li · K. P. Ananthapadmanabhan · Reinhold H. Dauskardt

Received: 30 March 2007 / Accepted: 8 May 2007 / Published online: 17 July 2007

Abstract Time-dependent intercellular delamination behavior of human stratum corneum (SC) is explored. We demonstrate that SC is susceptible to such time-dependent subcritical delamination at loads below the critical delamination energy. Hydration of the SC together with chemical treatments using selected surfactants were shown to affect both critical and subcritical delamination behavior. Increased tissue hydration resulted in accelerated delamination growth rates consistent with behavior anticipated from critical delamination testing. Chemical treatments including 10% wt/wt sodium dodecyl sulfate (SDS) and chloroform-methanol (2:1 v:v) soaks that remove lipid were shown to suppress growth rates compared to untreated controls. Possible mechanisms for subcritical delamination involving *extrinsic* mechanisms of moisture-assisted reaction process at the intercellular delamination tip or *intrinsic* mechanisms involving kinetic relaxation processes in the SC are discussed.

Abbreviations

SC	Stratum corneum
DCB	Double-cantilever beam
RH	Relative humidity
AAS	Amidosulfosuccinate
APG	Alkyl polyglucoside
CMT	Chloroform-methanol treated
SDS	Sodium dodecyl sulfate

K. S. Wu
Department of Mechanical Engineering, Stanford University, Stanford, CA 94305, USA

J. Li · R. H. Dauskardt (✉)
Department of Materials Science and Engineering, Stanford University, 416 Escondido Mall, Bldg 550, Rm 550G, Stanford, CA 94305-2205, USA
e-mail: dauskardt@stanford.edu

K. P. Ananthapadmanabhan
Unilever Research and Development, Trumbull, CT 06611, USA

Introduction

The stratum corneum (SC) serves as a mechanical and semipermeable chemical barrier between the body and the surrounding environment. We recently reported on the intercellular delamination behavior of SC to quantify the cohesive properties that maintain the mechanical integrity of this epidermal layer [1, 2]. The critical delamination energy, G_c [J/m^2], measured in terms of the applied strain energy release rate, G, was shown to vary significantly with SC hydration, temperature, and chemical treatment. Such conditioning and treatment affects the intercellular lipids and cellular proteins (e.g. keratin–keratin interactions) and their effects on intercellular delamination energies were quantified. The progressive degradation of corneosomes, or structural protein linkages, between SC cells toward the outer skin surface was also shown to result in reduced intercellular delamination energy using a modified version of the delamination technique [2]. The degraded corneosomes are associated with the continual renewal of SC in which exterior cells are replaced by less mature interior cells [3–8]. These studies, however, did not address the possibility of time-dependent delamination behavior.

Time-dependent delamination or cracking can provide useful insights into the kinetic bond rupture or molecular separation process. In some materials, such cracking is

associated with a chemical reaction that occurs between strained crack tip bonds and an environmental species such as H_2O that leads to bond rupture and crack advance [9]. In other materials, inherent creep or relaxation processes at the crack tip may lead to time-dependent material separation and crack advance [10, 11]. The phenomena is often referred to as *subcritical* cracking or delamination since it occurs at $G < G_c$, that is, at applied loads lower than those required for fracture in the absence of an environmental species or inherent relaxation process. Some materials exhibit no detectable subcritical cracking. In the case of SC no studies have reported on time-dependent intercellular delamination.

In the present study we demonstrate that SC is susceptible to subcritical delamination for applied $G < G_c$. Intercellular delamination growth rates, v, were characterized in selected moist air environments. We employed methods recently applied to measure subcritical delamination behavior in thin-film and layered structures for nanoscience and biomedical applications [9, 12–16]. Delamination growth rates were shown to be a strong function of the applied G resulting in a characteristic v–G curve. Conditioning of the SC tissue by changing hydration content and chemical treatments using surfactants were demonstrated to affect both critical and subcritical delamination behavior. Increasing SC hydration is shown to accelerate delamination growth rates consistent with behavior anticipated from critical delamination testing. Chemical exposure including 10% wt/wt sodium dodecyl sulfate (SDS) and chloroform-methanol (2:1 v:v) soaks that remove lipid suppressed growth rates compared to untreated controls. These treatments have been shown previously to affect lipid content and fluidity [4, 17]. Measured subcritical delamination behavior as a function of treatment is interpreted in terms of changes to SC microstructure and constituents.

Materials and methods

Tissue preparation

Human cadaver SC tissue was isolated from two female Caucasian donors, 57 and 101 years of age, from the thigh. Epidermal tissue was separated from dermis by immersion of donor tissue cleared of adipose tissue in a 35 °C water bath for 10 min followed by a 1 min soak at 60 °C and subsequent mechanical separation from the dermis using a flat-tipped spatula. Stratum corneum was isolated from underlying epidermis by soaking in a trypsin enzymatic digest solution (0.1% wt/wt in 0.05 M, pH 7.9 Tris buffer) at 35 °C for 120 min. During separation, the orientation of the outer SC surface was recorded. The isolated SC was rinsed with room temperature water and allowed to dry on filter paper (Grade 595 General-Purpose Filter Paper, Schleicher & Schuell MicroScience GmbH, Dassel, Germany) then removed and stored in ambient conditions of 18–23 ± 0.8 °C and 35–55 ± 2% relative humidity (RH) (Dickson TM325 Temperature & Humidity Data Logger, Addison, Illinois). Comparative tests were performed on single donor tissue specimens to reduce variability within test sequences. During separation, orientation of the outer SC surface was recorded.

To vary SC hydration, isolated tissue was exposed to environments with different RH values at ambient temperature (18–23 °C). A portion of the SC was placed in an enclosure held at 40% RH while additional SC was placed in another enclosure along with an open container of water to create a 100% RH environment to increase SC moisture content. The tissue was allowed to equilibrate for at least 24 h prior to fabrication of test specimens.

For comparison, SC, 60×60 mm^2, was chloroform-methanol treated (CMT) to delipidize the structure with a 120 min 30 mL chloroform:methanol (2:1 by volume) soak followed by two 30 min 30 mL water rinses. Additional tissue was treated in selected surfactant solutions to examine their effects on SC mechanical integrity. These specimens of SC 30×50 mm^2 were immersed in 100 mL of 10% wt/wt H_2O solutions of alkyl amidosulfosuccinate (AAS), alkyl polyglucoside (APG), and SDS for 18 h, then rinsed with distilled water and dried on filter paper. During treatment of SC, the solution pH values were pH 5.2, 8.1–8.7, and 7 ± 0.1 (Accumet Research AR25 Dual Channel pH/Ion Meter, Accumet Research, Fisher Scientific, Fair Lawn, NJ) for each treatment, respectively. These surfactant solutions have been shown to cause varying levels of lipid and protein damage as indicated in a comparative manner in Table 1.

Note that our previous studies have revealed that donor age and body location has an effect on measured delamination behavior [1, 2]. In the present study we compare results from single donors to negate these variations.

Delamination energy measurements

The fracture mechanics technique developed to measure the delamination energy of SC tissue has been described elsewhere [1]. Briefly, specimens were prepared by adhering SC tissue between two elastic substrates of polycarbonate (Hyzod® GP, Sheffield Plastics Inc., Sheffield, Massachusetts) with cyanoacrylate adhesive (Instant Krazy Glue© Gel, Elmer's Products Inc., Columbus, Ohio) to form a double-cantilever beam (DCB) fracture mechanics specimen as shown in Fig. 1. The substrate dimensions of $40 \times 10 \times 2.88$ mm^3 were selected to ensure elastic deformation and the valid application of linear elastic fracture mechanics.

Table 1 Table of showing SC tissue treatments, their relative protein and lipid damaging properties, and critical and subcritical delamination failure parameters

Treatment	Protein damage	Lipid damage	G_c (J/m^2)	Slope, m (da/dt/J/m^2)	G_{TH} (J/m^2)
Control (25 °C, 45% RH)	–	–	3.6–6.0	2.7 ± 0.3	1.9–2.9
Hydrated (25 °C, 100% RH)	–	–	1.1–2.4	9.1 ± 4.1	–
CMT	Low	High	6.9–8.0	2.8	4.8–5.7
SDS	High	Medium	7.7	2.9	4.7
APG	Low	Medium	1.4–5.9	5.0 ± 4.2	1.0
AAS	Low	Low	1.6–2.7	5.7 ± 3.6	0.7–1.5

Values accurate within ±5%

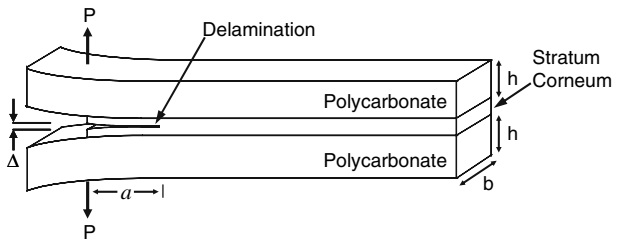

Fig. 1 Fracture mechanics DCB specimen geometry illustrating relevant loading parameters (P, Δ), delamination extension, a, as measured from loading axis points and relevant specimen dimensions (b = 10 mm, h = 2.88 mm, length = 40 mm)

The specimens were mounted at the SC-free end via loading tabs in an adhesion test system (Delaminator Test System v4.0, DTS Company, Menlo Park, CA) with a computer controlled DC servoelectric actuator operated in displacement control. The adhesion test apparatus and DCB specimens were placed in an environmental chamber (Model LH-6, Associated Environmental Systems, Ayer, Massachusetts or Model ZH-16-2-H/WC, Cincinnati Sub-Zero [CSZ], Cincinnati, Ohio) to control test environment. Specimens were loaded in Mode I tension. Several critical delamination energy (G_c) values were measured for each DCB specimen and tested using either 2 or 5 μm/s displacement rates during delamination extension with corresponding loads measured with a 222 N load cell. The delamination length, a, was measured from recorded load-displacement curves, P–Δ, and their elastic compliance relationship:

$$C = \frac{\Delta}{P} = \frac{2}{3}\frac{(a+0.64h)^3}{E'I} \tag{1}$$

where C is the DCB specimen compliance, P is the load, Δ/2 is the corresponding displacement of each beam from its original position at the loading point, $E' = E/(1-V^2)$ is the plane strain Young's modulus for the polycarbonate, v is Poisson's ratio, $I = bh^3/12$ is the area moment of inertia, b is the polycarbonate substrate width, and h is the height of each polycarbonate beam. For the present specimens, the values of E and v for the polycarbonate were 2.379 and 0.38 GPa, respectively. By measuring the critical load, P_C, and the delamination length, a, at incipient delamination extension, the delamination resistance, G_c, was determined from critical values of the strain energy release rate, G [18, 19]:

$$G = \frac{12P^2a^2}{b^2h^3E'}\left(1+\frac{\sqrt{5}}{2}\frac{h}{a}+\frac{1}{2}\left(\frac{h}{a}\right)^2\right) \tag{2}$$

More detailed methods and results for critical delamination energies as a function of treatment and conditioning are described elsewhere [1].

Subsequently, after creation of a uniform delamination front during critical delamination testing, the DCB specimens were unloaded. The beam ends were then displaced at a constant rate of 5 μm/s while monitoring the load such that delamination growth was not observed to occur. Once a load below the anticipated critical load, P_C, to initiate delamination growth was obtained, the displacement of the beams was stopped, and the resulting subcritical load was monitored as a function of time. The measured loads were observed to decrease with time as the delamination propagated through the specimen, increasing the compliance of the DCB structure. From the compliance measured during initial displacement of the DCB substrates prior to holding constant displacement, the initial delamination length, a_i, can be determined by rearranging Eq. 1 to yield the following expression for delamination length:

$$a = \left(\frac{\Delta}{P}\cdot\frac{E'bh^3}{8}\right)^{1/3} - 0.64h \tag{3}$$

During the load-relaxation component of the subcritical test, the displacement, Δ, is held fixed with time and knowledge of the initial debond length, a_i, and peak load, P_i, from the initial loading of the specimen, allows calculation of the delamination length as a function of time:

$$a(t) = a_i \left(1 + 0.64 \cdot \frac{h}{a_i}\right)\left(\frac{P_i}{P(t)}\right)^{1/3} - 0.64h \quad (4)$$

The delamination growth velocity can be calculated by taking the time derivative of the above expression:

$$\frac{da}{dt} = -\frac{a_i}{3}\left(1 + 0.64 \cdot \frac{h}{a_i}\right)\left(\frac{P_i^{1/3}}{P(t)^{4/3}}\right)\frac{dP}{dt} \quad (5)$$

Subcritical values of G are calculated from the measured loads corresponding calculated delamination lengths (Eq. 2). Knowledge of these two parameters allows one to plot delamination growth rate ($v = da/dt$) as a function of the applied strain energy release rate, G, also known as v–G curves. A typical v–G curve is shown in Fig. 3.

For the above calculations, the resultant error for the calculated crack length, a, is <±1% and for delamination resistance values, G, and delamination growth velocity, da/dt, <±5%. In particular, instrument error associated with compliance, C, and geometric dimension measurements, b and h were <±0.2% for the values measured.

Results

Load-relaxation data for SC conditioned at 18–23 °C, 40% RH and tested in a 25 °C, 45% RH environment is shown in Fig. 2. The data clearly show that significant load-relaxation has occurred, and corresponding calculation of delamination length revealed subcritical delamination growth with time. The initial delamination length, a_i, and peak load, P_i, used to calculate delamination length and growth rate with time are indicated. Analysis of the load-relaxation data using Eqs. 2 and 5 allowed determination of delamination growth rates as a function of applied G as shown in Fig. 3. The corresponding critical delamination energy, G_c, is included for comparison. Delamination growth rates were characterized over nearly five orders of magnitude, and were clearly sensitive to the applied loads. Intermediate growth rates in the range of 10^{-8}–10^{-5} m/s exhibited an exponential dependence on G. Alternatively, a power-law relationship of the form $da/dt = C \cdot G^m$ can be employed to characterize the intermediate delamination growth rates, where C and the exponent m are constants dependent on tissue condition and testing environment. Threshold behavior for applied loads approaching a threshold applied strain energy release rate, G_{TH}, was clearly apparent at low growth rates approaching 10^{-9} m/s. Delamination is presumed dormant at applied G less than G_{TH}. Not all materials exhibit a clear threshold load for crack or debond growth as reported in a recent study of debonding of a polymer/inorganic interface [20]. For both hydration and surfactant treated SC, a summary of salient treatments, cohesive delamination energy, G_c, values and parameters for

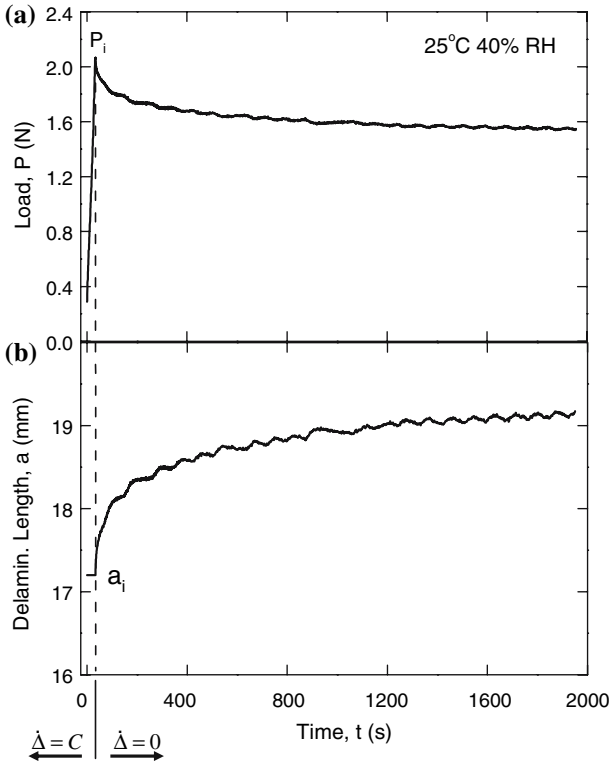

Fig. 2 Load-relaxation data illustrating for SC conditioned at 18–23 °C, 40% RH and tested in a 25 °C, 45% RH environment showing (**a**) initially increasing load at constant displacement rate ($\dot{\Delta} = C$) followed by load decrease with time once displacement is fixed ($\dot{\Delta} = 0$), and (**b**) delamination length as a function of time calculated from specimen compliance. Corresponding subcritical curve shown in Fig. 3

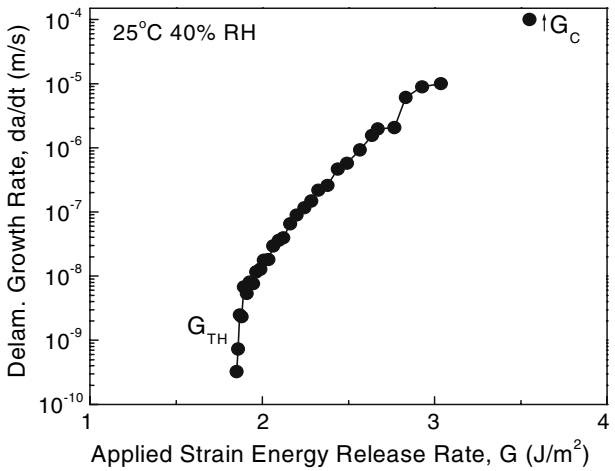

Fig. 3 Typical delamination growth rate (da/dt) versus applied strain energy release rate (G) for SC conditioned at 18–23 °C, 40% RH and tested in a 25 °C, 45% RH environment showing threshold behavior (G_{TH}) and critical delamination energy values (G_c)

characterization of subcritical delamination behavior are presented in Table 1.

Subcritical delamination as a function of tissue hydration

The effects of preconditioning the SC on delamination growth rate behavior are shown in Figs. 4 and 5. The curves in Fig. 4 show behavior for specimens from the same tissue sample conditioned in selected RH air environments at ambient temperatures 18–23 °C for at least 24 h followed by testing in similar RH environments at 25 °C. Data presented in Fig. 5 includes similarly prepared specimens from another tissue sample as well as specimens preconditioned at one RH and tested in a different RH. Debond growth rate curves for tissue conditioned and tested at either 40–45% RH or 90–100% RH exhibited well defined debond growth curves with evidence of debond growth thresholds, G_{TH}, at growth rates approaching 10^{-9} m/s. For each RH range examined, some scatter in the crack growth curves was apparent and is indicated by the shaded area in the figures. Such scatter is not uncommon for crack growth behavior and certainly not excessive for natural tissues. Increasing SC hydration with higher RH conditioning led to accelerated growth rates and steeper slopes of the delamination growth curves. Critical G_c values were also found to decrease with increasing hydration as previously reported [1].

The effects of testing a specimen preconditioned in one RH environment and tested in a different RH environment are shown in Fig. 5. The specimen preconditioned at 40% RH and tested in a 92% RH environment exhibited intermediate growth rates in the same range as tissue conditioned and tested in a 40–45% RH environment. However, as the growth rates decreased, a plateau in the growth rate at approximately 6×10^{-9} m/s was apparent with little dependence on applied G. With decreasing loads, the growth rate remained relatively constant until G reached values typical for the 100% RH conditioned tissue. Growth rates then appeared to be consistent with those for the 100% RH conditioned tissue and the onset of a threshold was also apparent. The time the tissue was exposed to the higher humidity testing environment was approximately 2.6×10^4 s.

Tissue conditioned at 100% RH and tested in the drier 45% RH environment exhibited behavior essentially the same as that for specimens treated and tested at the higher RH. However after 4×10^3 s, the tissue was affected by the drier testing environment and exhibited some contraction that was evidenced by the measured load beginning to increase with time. This behavior invalidated the load relaxation analyses and the test was terminated at the last valid growth rate in the vicinity of 10^{-8} m/s.

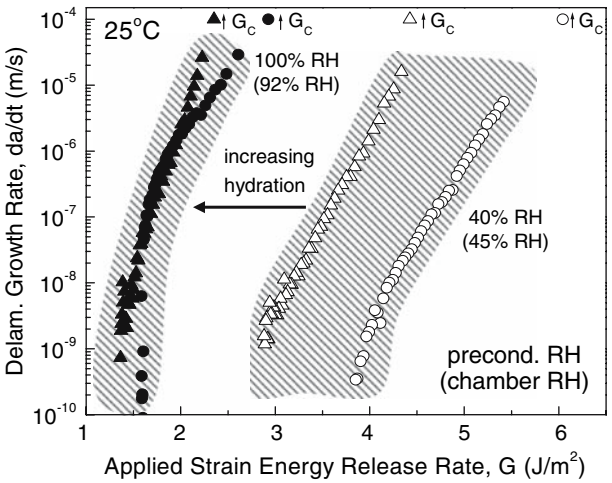

Fig. 4 Delamination growth rate (da/dt) versus applied strain energy release rate (G) for SC specimens conditioned in environments of different RH at ambient temperatures 18–23 °C and tested in environments with RH similar to their preconditioning values. Labels show the preconditioning RH and environmental test chamber RH in parentheses

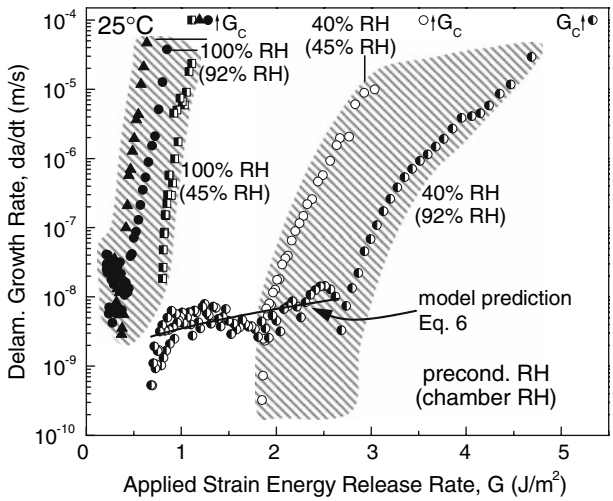

Fig. 5 Delamination growth rate (da/dt) as a function of applied strain energy release rate (G) showing SC preconditioned and tested in similar environments (filled and open points) and for specimens preconditioned at one RH and tested in an environment with different RH (half filled, half open points). Subcritical curves for 100% RH conditioned specimens are observed to plateau at lower strain energy release rates. Labels show the preconditioning RH and environmental test chamber RH in parentheses

Effects of tissue surfactant treatments

Delamination was performed on CMT, AAS, APG, and SDS treated tissue to examine the effects of these solutions on SC delamination growth rate behavior compared to that of untreated controls. These specimens were conditioned

and tested at 45% RH at ambient temperatures 18–23 °C and 25 °C, respectively. These data are presented in Fig. 6 with parameters listed in Table 1. The shapes of the delamination growth rate curves were similar to the untreated SC although the slope, and particularly the position of the v–G curves along the G-axis, exhibited a marked sensitivity to the tissue treatment. The curves all exhibited threshold behavior at low delamination growth rates. The harsh CMT and SDS surfactant treated tissue exhibited delamination growth rate curves at significantly higher G values compared to the untreated control, and the tissue treated in the milder surfactants, AAS and APG, exhibited curves at lower applied G values indicative of decreased resistance to delamination. Critical delamination energy values, G_c, exhibited similar trends with treatment to the time-dependent delamination curves.

Discussion

Susceptibility to subcritical delamination

The data presented in the present study demonstrates that SC tissue is susceptible to time-dependent intercellular delamination growth under load in moist environments. Not all materials or interfaces exhibit such time dependent delamination or cracking at applied loads less than the fracture energy G_c.

The observed behavior may be associated with a chemical reaction that occurs between strained crack tip bonds and an environmental species such as H_2O which leads to bond rupture and crack advance [9, 14–16]. This type of environmentally assisted cracking generally has characteristic features of the resulting v–G curve. Intermediate growth rates in the range of 10^{-8}–10^{-5} m/s are strongly sensitive to applied G, the activity of the environmental species and temperature, indicative of the environmentally assisted reaction kinetics associated with the crack tip bond rupture process. Further decreases in G often result in threshold behavior below approximately 10^{-9} m/s where crack growth rates decrease below detectable limits. At higher growth rates, a transport-limited region largely independent of G is characterized by a plateau in the v–G curve [9, 14–16]. We did not observe a transport limited region in the present study, but such behavior is often observed at higher crack growth rates, which we did not characterize. With still further increases in applied loads where G approaches G_c fracture occurs at high crack growth rates and is largely independent of environmental test conditions.

Time dependent fracture may also be related to inherent creep or relaxation processes that occur in a process zone surrounding the crack tip that lead to material separation and crack advance. Such behavior has been reported for metals, inorganic, and organic materials [10, 11]. In the case of polymers, the time dependence of crack growth results from viscoelastic deformation in the crack tip process zone which is dependent on both testing temperature and crack growth rate [11]. While we were not able to unambiguously establish the precise time dependent debonding mechanism in the present study, the intercellular separation process that occurs during delamination of SC involving separation of intercellular lipids and corneodesmosomes suggests that the latter process involving an inherent time dependent molecular separation process is more likely. We note also that the SC does not contain atomic bonds like silanol bonds in inorganic glasses that are particularly sensitive to moisture adsorption and associated bond cleavage. Organic molecules containing carbon backbones are generally insensitive to cleavage by H_2O or OH molecules in moist environments and therefore typically insensitive to environmentally assisted cracking.

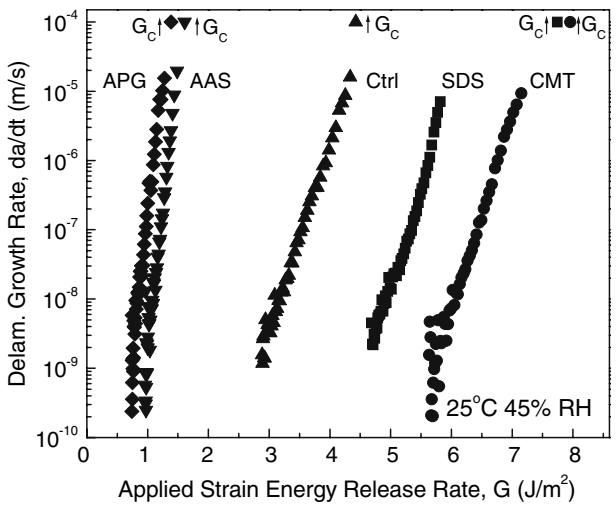

Fig. 6 Effect of chemical treatments on critical and subcritical delamination behavior. Critical and subcritical delamination energy measurement results for various pH and surfactant treatments (SDS: sodium dodecyl sulfate (10% wt/wt); CMT: chloroform-methanol (2:1 v:v) treatment; APG: alkyl polyglucoside (10% wt/wt); AAS: alkyl amidosulfosuccinate (10% wt/wt))

Hydration effects

The reduction in critical delamination energies, G_c, with SC hydration (Figs. 4, 5) is consistent with prior examinations of critical delamination energy values [1, 2]. The effects of hydration on SC components are numerous including corneocytes swelling and the presence of water pooling between cells [21, 22], disruption of intercellular lipid lamellae [23, 24], and even the degradation of corneodesmosomes [7, 21]. We discussed the decreased

intercellular delamination energy G_c values with increased SC hydration in terms of increased lipid mobility and possible intercellular boundary separation by the presence of water which would lower the measured G_c [1, 2].

The same mechanisms leading to decreased G_c values with increasing SC hydration likely affect the observed time-dependent delamination behavior and lead to v–G curves shifted to lower values of applied G. Alternatively, for a given value of applied G, delamination growth rates would be significantly faster with increased SC hydration. The steeper slopes of the v–G curves with increased SC hydration shown in Fig. 5 (crack growth exponents m in Table 1) further highlight the structurally degrading effect of tissue hydration. Delamination growth rates were more sensitive to changes in applied G for highly hydrated SC compared to the less hydrated specimens.

The effects of plastic energy dissipation in the SC layer are not likely to contribute significantly to delamination energy which has been linked more strongly to the intercellular separation process [1, 2]. The observation that increased hydration accelerates delamination growth rates further corroborates this notion. If plasticity played an important role in delamination behavior, growth rates would be expected to decrease with increasing hydration (i.e. v–G curves would shifted to higher values of applied G compared to drier specimens) due to increased tissue plastic deformation associated with the lower yield stress reported for hydrated SC [1].

To elucidate the possible mechanisms associated with time dependent delamination and to probe the effects of changing the H_2O activity in the testing environment, v–G curves were measured for several specimens preconditioned at either a low or high humidity and then tested in the opposite humidity environment. The results shown in Fig. 5 clearly reveal that changes to the testing environment RH do not cause changes in the v–G curves for delamination growth rates greater than 10^{-8} m/s. The insensitivity to environmental RH suggests that time dependent delamination behavior is determined by the SC hydration rather than that of the testing environment. This suggests that the mechanism of time-dependent intercellular delamination is not controlled by a chemical reaction process similar to silanol bond cleavage in moist environments reported in silica glasses. This mechanism would lead to significant sensitivity to the moisture content of the test environment.

Only at low growth rates less than 10^{-8} m/s when the low humidity conditioned tissue was exposed to the higher humidity testing environment for longer times did the growth rate behavior begin to approach that of SC conditioned in the higher humidity environment. This is clearly apparent for the SC preconditioned at 40% RH and tested in a 92% RH environment (Fig. 5). At low growth rates the SC near to the crack tip absorbs water from the testing environment as shown schematically in Fig. 7 and growth rates eventually approach that of the higher humidity conditioned SC. When hydrated tissue is tested in a dry environment, the opposite behavior involving diffusion of water out of a zone surrounding the delamination would occur. This phenomenon represents a coupled rate dependent process where the rate of moisture diffusion competes with the delamination growth rate. When the delamination growth rate is sufficiently high (for the present SC and temperature $>10^{-8}$ m/s) the delamination propagates faster than moisture diffusion can equilibrate the tissue surrounding the delamination tip to the testing environment. At lower growth rates the SC at the delamination tip becomes equilibrated to the moisture content of the testing environment.

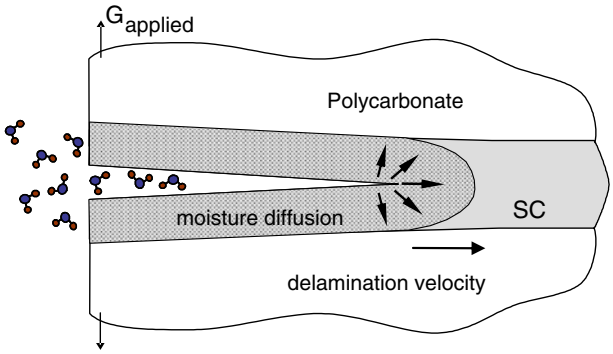

Fig. 7 Schematic illustration of intercellular delamination in a DCB specimen showing diffusion of moisture from the test environment into a region surrounding the delamination

The above observations suggest that the intrinsic SC hydration dominates the time-dependent intercellular separation process and delamination growth rates. In a recent study, the debonding behavior of weakly bound interfaces between polymer layers and an under laying elastic substrate were characterized in moist environments [20]. At low growth rates, a similar plateau was observed where debond growth rates were characterized by a weak dependence on applied G, a strong dependence on moisture activity, and the absence of a measurable threshold. The mechanism of debonding was associated with the diffusion of moisture in the polymer layer to the interface where it weakens the interface and gives rise to time dependent delamination. The weak dependence on applied G is related to the stress dependent diffusion of water that is well known in polymers. Incorporating the stress dependent diffusion constant of water in the polymer later into a debond growth model allowed the following prediction for the debond growth rate:

$$\frac{da}{dt} = C\, a_{H_2O} D_0 \exp\left(\frac{-E_d + \alpha\sqrt{G}}{RT}\right) \quad (6)$$

where C a constant that includes the concentration of reactant molecules, the interfacial bond length and areal bond density, a_{H_2O} is the moisture activity, D_0 is the pre-exponential diffusion coefficient of water in the polymer, E_d is the activation energy for diffusion, α is a constant involving the activation volume associated with the diffusion process, R the universal gas constant, and T the temperature in Kelvin. The constant α/RT in the exponential was found to be approximately 1 $kJ^{1/2}$ m/mol. While is it premature to attempt a similar detailed fit of the above model to the present study where the structure of the intercellular delamination path including details of the lipid and corneodesmosome bond length and areal density are not known, it is nevertheless instructive to note that the observed plateau in growth rates is likely related to a very similar mechanism involving moisture diffusion through the SC layer. If that is the case, then it is also possible that the moisture diffusion will exhibit the same stress dependence observed in other organic polymer materials. We should then expect to observe a similar weak dependence of growth rates in the plateau region on the applied G as predicted by Eq. 6. Using a simplified form of Eq. 6 we find that a best fit to the data yields a value of α/RT = 1.5 $kJ^{1/2}$ m/mol which is in close agreement with the previous value of α for weakly bound polymer interfaces, and further that the model captures the plateau growth rate dependence on G very well. In fact, the successful application of the stress-dependent transport model suggests that like other organic polymer materials, water diffusion in SC may well be stress dependent.

Chloroform-methanol and surfactant effects

When exposed to chemical treatments, SC exhibits significant changes in delamination behavior as seen in Fig. 6 and quantified in Table 1 for both critical and subcritical measurements. The treatments used to condition SC in these subcritical tests have been shown to damage protein and lipids structures to varying degrees as compared in Table 1. Chloroform-methanol extraction has been shown previously to remove the majority of intercellular lipids from SC tissue facilitating the direct apposition of unextracted lipids covalently bound to the cornified envelopes of adjacent corneocytes [4, 25–29]. The increased critical delamination energies of delipidized SC have been attributed to the interdigitation of opposing corneocyte envelope lipids [28, 30]. Only with extraction of the lamellae and envelope lipids is dissociation of SC tissue into individual cells observed, supporting this explanation [31]. Through thickness multiple delamination tests on CMT SC has indicated that the extraction is pervasive throughout the SC layer leading to overall increases in delamination energies compared to untreated controls [2]. The strong surfactant quality of SDS likely plays a similar role in extracting intercellular lipids leading to increases in critical delamination energies.

Extending our knowledge of surfactant behavior on critical delamination energies to subcritical behavior, we find delamination growth rate curves shifted to higher G-values with strong surfactant treatments (Fig. 6) similar to trends observed between critical delamination energy values. The similar shapes of the v–G curves between untreated and treated specimens indicate that the mechanisms driving delamination growth are similar but that higher applied G values are required to facilitate activation of the kinetic processes leading to subcritical delamination growth. The similar behavior to reaction-controlled curves for treated delamination growth velocities as a function of G suggests that similar mechanisms to those seen in untreated SC may be occurring. The differences in subcritical curve positions along the G axis may be attributed to modifications of the intercellular material through which the debonding occurs. For the CMT and SDS treated SC, depletion of intercellular lipid bonds with strongly corneocyte envelope lipid interactions provides an obvious explanation of the increased G-values; however, the accelerated delamination rates that occur with exposure to milder surfactants (AAS and APG) cannot be explained in the same manner.

Examining the milder surfactant treatments, their critical delamination energies fall toward lower values than those of the untreated controls. These results suggest that these milder surfactants do not affect the SC in the same manner as the harsher surfactants. The results are surprising because any lipid extraction would be expected to cause increases in SC delamination energies while exposure to these solutions led to decreases. One competing mechanism that may explain the incongruous behavior is that of SC hydration content. While the described tests control external factors such as environmental RH, the actual water content of the SC may vary with treatment as water-holding capacity is modulated if hygroscopic natural moisturizing factor (NMF) content is changed in the system. Alternatively, the treatments may increase water holding capacity of the skin as is the case with glycerol which has been shown to absorb into SC and whose large water-holding capacity is well known [32, 33]. This effect of hydration may explain the decreases in delamination energies with AAS and APG treatment but require further examination to provide evidence of these effects. The subcritical data, however, faithfully track with the critical values and exhibit similar behavior to that of untreated and harsher surfactant-treated SC.

Conclusions

We demonstrate that SC is susceptible to time-dependent subcritical delamination at loads below the critical delamination energy. Increased hydration has been shown to accelerate delamination growth rates for a given applied strain energy release rate; however, the SC is sensitive only to its hydration state and not to that of the external environment as shown from tests in which specimens are preconditioned in one environment with set RH and tested in another with different RH. Chemical treatments were demonstrated to shift the subcritical growth rate curves along the applied strain energy release rate axis compared to untreated controls. The slope of the chemically treated SC growth rate curve was similar to the untreated specimens preconditioned and tested at similar temperature and RH values. The delamination growth rate behavior was characteristic of classical chemical reaction rate or creep crack growth controlled behavior without evidence of a transport controlled region. At low growth rates, specimens preconditioned in a relatively dry environment (45% RH) and tested in a humid environment (92–100% RH) exhibited a plateau like growth rate behavior as a function of applied loads that appears related to a stress dependent moisture diffusion process in the SC. Based on the sensitivity of intercellular delamination growth rates to tissue conditioning and insensitivity to the moisture content of the external environment, a mechanism involving inherent creep or relaxation processes appeared more likely. We believe that the research demonstrates that the time dependent delamination of human SC provides a potentially sensitive indication of the effects of tissue condition and treatment. It may therefore have important application in the screening of treatments.

Acknowledgments This work was supported by a grant from Unilever Research and Development (Edgewater, NJ; Trumbull, CT).

References

1. Wu KS, van Osdol WW, Dauskardt RH (2006) Biomaterials 27(5):785
2. Wu KS, Stefik MM, Ananthapadmanabhan KP, Dauskardt RH (2006) Biomaterials 27(34):5861
3. Chapman SJ, Walsh A (1990) Arch Dermatol Res 282(5):304
4. Chapman SJ, Walsh A, Jackson SM, Friedmann PS (1991) Arch Dermatol Res 283(3):167
5. Lundstrom A, Serre G, Haftek M, Egelrud T (1994) Arch Dermatol Res 286(7):369
6. Walsh A, Chapman SJ (1991) Arch Dermatol Res 283(3):174
7. Rawlings A, Harding C, Watkinson A, Banks J, Ackerman C, Sabin R (1995) Arch Dermatol Res 287(5):457
8. Simon M, Bernard D, Minondo AM, Camus C, Fiat F, Corcuff P et al (2001) J Invest Dermatol 116(1):23
9. Wiederhorn SM (1967) J Am Ceram Soc 50(8):407
10. Riedel H (1987) Fracture at high temperatures. Springer-Verlag, Berlin, New York
11. Bradley W, Cantwell WJ, Kausch HH (1997) Mech Time-dependent Mater 1(3):241
12. Ohashi KL, Dauskardt RH (2000) J Biomed Mater Res 51(2):172
13. Ohashi KL, Yerby SA, Dauskardt RH (2001) J Biomed Mater Res 54(3):419
14. Guyer EP, Dauskardt RH (2005) J Mater Res 20(3):680
15. Guyer EP, Dauskardt RH (2004) Nat Mater 3(1):53
16. Lane MW, Snodgrass JM, Dauskardt RH (2001) Microelectron Reliab 41(9–10):1615
17. Ananthapadmanabhan KP, Lips A, Vincent C, Meyer F, Caso S, Johnson A et al (2003) Int J Cosmet Sci 24:103
18. Kanninen MF (1973) Int J Frac 9(1):83
19. Ohashi KL, Romero AC, McGowan PD, Maloney WJ, Dauskardt RH (1998) J Orthop Res 16(6):705
20. Sharratt BM, Wang LC, Dauskardt RH (2007) Acta Mater 55(10):3601
21. Bouwstra JA, de Graaff A, Gooris GS, Nijsse J, Wiechers JW, van Aelst AC (2003) J Invest Dermatol 120(5):750
22. van Hal DA, Jeremiasse E, Junginger HE, Spies F, Bouwstra JA (1996) J Invest Dermatol 106(1):89
23. Warner RR, Stone KJ, Boissy YL (2003) J Invest Dermatol 120(2):275
24. Warner RR, Boissy YL, Lilly NA, Spears MJ, McKillop K, Marshall JL et al (1999) J Invest Dermatol 113(6):960
25. Sznitowska M, Janicki S, Williams A, Lau S, Stolyhwo A (2003) J Pharm Sci 92(1):173
26. Swartzendruber DC, Wertz PW, Madison KC, Downing DT (1987) J Invest Dermatol 88(6):709
27. Wertz PW, Madison KC, Downing DT (1989) J Invest Dermatol 92(1):109
28. Wertz PW, Swartzendruber DC, Kitko DJ, Madison KC, Downing DT (1989) J Invest Dermatol 93(1):169
29. Wertz PW, Swartzendruber DC, Madison KC, Downing DT (1987) J Invest Dermatol 89(4):419
30. Stewart ME, Downing DT (2001) J Lipid Res 42(7):1105
31. Smith WP, Christensen MS, Nacht S, Gans EH (1982) J Invest Dermatol 78(1):7
32. Reiger MM, Deem DS, Skin Moisturizers II (1974) J Soc Cosmet Chem 25:253
33. Froebe CL, Simion FA, Ohlmeyer H, Rhein LD, Mattai J, Cagan RH et al (1990) J Soc Cosmet Chem 41:51